Aged-senescent cells contribute to impaired heart regeneration

Fiona C. Lewis-McDougall[1], Prashant J. Ruchaya[1], Eva Domenjo-Vila[1], Tze Shin Teoh[1], Larissa Prata[2], Beverley J. Cottle[1], James E. Clark[3], Prakash P. Punjabi[4], Wael Awad[5], Daniele Torella[6], Tamara Tchkonia[2], James L. Kirkland[2], Georgina M. Ellison-Hughes[1]

[1]School of Basic and Medical Biosciences, Faculty of Life Sciences & Medicine, Kings College London, London, UK; [2]Robert and Arlene Kogod Center on Aging, Mayo Clinic College of Medicine, Rochester, Minnesota, USA;[3]School of Cardiovascular Medicine & Sciences, Faculty of Life Sciences & Medicine, Kings College London, London, UK; [4]National Heart and Lung Institute, Imperial College London, London, UK; [5]Barts Health NHS Trust, London, UK; [6]Molecular and Cellular Cardiology, Department of Medical and Surgical Sciences, Magna Graecia University, Catanzaro, Italy.

Correspondence should be addressed to G.M.E-H (georgina.ellison@kcl.ac.uk)

Abstract

Aging leads to increased cellular senescence and is associated with decreased potency of tissue-specific stem/progenitor cells. Here we have done an extensive analysis of cardiac progenitor cells (CPCs) isolated from human subjects with cardiovascular disease ~~(n=119)~~, aged 32-86 years. In aged subjects (>74 years old) over half of CPCs are senescent ($p16^{INK4A}$, SA-β-gal, DNA damage γH2AX, telomere length, Senescence-Associated Secretory Phenotype (SASP)), unable to replicate, differentiate, regenerate or restore cardiac function following transplantation into the infarcted heart. SASP factors secreted by senescent CPCs renders otherwise healthy CPCs to senescence. Elimination of senescent CPCs using senolytics abrogates the SASP and its debilitative effect *in vitro*. Global elimination of senescent cells in aged mice (INK-ATTAC or wildtype mice treated with D+Q senolytics) *in vivo* activates resident CPCs (0.23±0.06% *vs.* 0.01±0.01% vehicle; $p<0.05$) and increased the number of small, proliferating Ki67-, EdU-positive cardiomyocytes (0.25±0.07% *vs.* 0.03±0.03% vehicle; $p<0.05$). Therapeutic approaches that eliminate senescent cells may alleviate cardiac deterioration with aging and ~~rejuvenate~~ restore the regenerative capacity of the heart.

Formatted: Font: Italic

Formatted: Font: Italic

Introduction

Ageing is the greatest risk factor for many life-threatening disorders, including cardiovascular diseases, neurodegenerative diseases, cancer, and metabolic syndromes (St Sauver et al. 2015). Aging leads to increased cellular senescence in a number of tissues and is frequently associated with increased expression of the senescence biomarker, $p16^{Ink4a}$ (also known as Cdkn2a), resistance to apoptosis, and impaired proliferation and tissue regeneration (Jeyapalan and Sedivy, 2008; Sharpless and DePinho, 2007; Krishnamurthy et al. 2004). Senescent cells disrupt tissue structure and function through their senescence-associated secretory phenotype (SASP), consisting of pro-inflammatory cytokines, chemokines, ~~and~~ ECM-degrading proteins, and other factors, which have deleterious paracrine and systemic effects (Tchkonia et al. 2013; Xu et al. 2015, ~~eLIFE~~; Xu et al. 2015, ~~PNAS~~). Remarkably, even a relatively low abundance of senescent cells (10-15% in aged primates) is sufficient to cause tissue dysfunction (Herbig et al. 2006).

To test whether senescent cells are causally implicated in age-related dysfunction and whether their removal is beneficial, J. L. Kirkland, T. Tchkonia, ~~D. Baker (Mayo),~~ J. van Deursen (Mayo), D. Baker (Mayo) and colleagues made use of a promoter for the biomarker for senescence, $p16^{INK4a}$, and an inducible "suicide" gene designed by P. Scherer *et al.* (Pajvani et al. 2005) to develop a novel transgene, INK-ATTAC, to permit inducible elimination of $p16^{INK4a}$-positive senescent cells upon administration of a drug (AP20187) (Baker et al. 2011). In these mice, eliminating a relatively small proportion (~30%) of senescent cells extends health span and prevents the development of multiple age-related morbidities in both progeroid and normal, chronologically aged mice (Baker et al. 2011; Roos et al. 2016; Farr et al. 2017; Ogrodnik et al. 2017; Schafer et al. 2017; Xu et al. 2018). Moreover, late life clearance attenuated the progression of already established age-related disorders (Xu et al. 2018). To be applicable to humans, Kirkland and collaborators have identified a new class of drugs named senolytics in work that paralleled, but was not dependent on development of INK-ATTAC mice. Through exploiting senescent cells' dependence on specific pro-survival pathways, senolytics specifically kill senescent cells without affecting proliferating or quiescent, differentiated cells (Kirkland and Tchkonia, 2015; Kirkland et al. 2017; Kirkland and Tchkonia, 2017). Recent studies have documented senolytic drugs for the selective clearance of senescent cells from 'aged' tissues, which led to delayed acquisition of age-related pathologies (Tchkonia and Kirkland, 2018). Recently, the Kirkland lab has demonstrated that transplanting relatively small numbers of senescent

preadipocyte cells into young (6 month old) mice causes persistent physical dysfunction, measured through maximal speed, hanging endurance and grip strength, 1 month after transplantation. Transplanting even fewer senescent cells into older (17 month old) recipients had the same effect and reduced survival, indicating the potency of senescent cells in shortening health- and lifespan. Intermittent oral administration of the senolytics, dasatinib (D), a FDA-approved tyrosine kinase inhibitor, and quercetin (Q), a flavonoid present in many fruits and vegetables, to senescent cell-transplanted young mice and naturally aged mice alleviated physical dysfunction and increased post-treatment survival by 36% while reducing mortality hazard to 65% (Xu et al. 2018). Altogether these data indicate that cellular senescence is causally implicated in generating age-related phenotypes and that systemic removal of senescent cells can prevent or delay tissue dysfunction, physical dysfunction and extend health- and lifespan.

Like other organs, the adult mammalian heart has the capacity, albeit low, to self-renew cardiomyocytes over the human lifespan (Bergmann et al. 2009), and genetic fate mapping models show that one source of new cardiomyocytes are a population of resident stem cells (Ellison et al. 2013; Hsieh et al. 2007). Multiple labs have shown the mammalian heart, including human, to harbour self-renewing, clonogenic, multipotent cardiac stem and progenitor cells (CSCs or CPCs; abbreviated hereafter as CPCs) with regenerative potential *in vivo* (Ellison-Hughes and Lewis, 2017; Vicinanza et al. 2017). An undisputed mechanism of action of CPC transplantation into the infarcted myocardium is their secretome reparative potential, which through acting in a paracrine manner improves cardiomyocyte survival, limits fibrosis, induces angiogenesis, new cardiomyocyte formation and restores cardiac function (Broughton et al. 2018) .

Our lab has defined the CPC population to be Sca-1^{pos}/c-kit^{pos}/CD31^{neg}/CD45 ^{neg}/Tryptase ^{neg} (Ellison et al. 2013; Vicinanza et al. 2017; ~~Ellison et al. 2011~~) distinguishing them from cardiac c-kit^{pos} endothelial (CD31^{pos}) and mast (CD45^{pos}/Tryptase^{pos}) cells. The CPCs are a rare population in the adult heart, with ~1% evidencing cardiomyogenic regeneration potential (Vicinanza et al. 2017). Recently, considerable confusion has emanated over the significant cardiomyogenic potential of CPCs purported using Kitcre Knockin or dual recombinases-mediated cell tracking mouse~~ice~~ models (van Berlo et al. 2014; ~~Sultana et al. 2015~~; Li et al. 2018). However, these models do not tag or specifically lineage trace the CPCs, neither have the investigators isolated, characterised or transplanted CPCs (according

Formatted: Highlight

Formatted: Highlight

to the Sca-1^{pos}/c-kit^{pos}/CD31^{neg}/CD45 ^{neg}/Tryptase ^{neg} phenotype given above) from these mice to test their stem cell and regenerative properties. Moreover, the c-kitCre null allele produced by Cre insertion fails to recombine the CPCs in the Kitcre mice and there is a severe defect in CPC myogenesis produced by the c-kit hemizygosity (Vicinanza et al. 2018).

Cardiac aging and pathology affects the activity and potency CPCs (Cesselli et al. 2011; Castaldi et al. 2017; Torella et al. 2004), which translates into a diminished capacity of the aged and diseased myocardium to maintain homeostasis, and repair and regenerate following injury (Ellison and Lewis et al. 20174). The aging *milieu* might therefore limit the success of cell transplantation therapies where the outcome is direct cardiogenic differentiation of transplanted cells and/or stimulation of endogenous regenerative mechanisms. As the majority of cardiovascular disease patients in need of regenerative therapies are of advanced age, regulation of CPC and cardiovascular aging/senescence is mission critical.

Here we have carried out an extensive analysis of CPCs in the human failing heart with advanced age and show the accumulation of senescent-CPCs, which exhibit diminished self-renewal, differentiation, and regenerative potential *in vivo*. We show that Senescent-CPCs have a SASP that negatively affects healthy non-senescent, cycling-competent CPCs, rendering them senescent. Clearing the senescent-CPCs using senolytics attenuates the SASP and its effect on promoting senescence *in vitro*. The effects of global elimination of senescent cells on the heart and its regenerative capacity have not been elucidated. We report novel data that show systemic elimination of senescent cells *in vivo* in aged mice using senolytics (D+Q) or using the 'suicide' transgene, INK-ATTAC with administration of AP20187, results in CPC activation and increased number of small, immature, proliferating EdU+ cardiomyocytes in the aged mouse heart.

Results

CPCs exhibit a senescent phenotype with increased age

Human CPCs were isolated from biopsies of right atria, obtained from subjects who had given informed consent before undergoing cardiac surgery (aortic disease, valve disease, coronary artery bypass graft (CABG), or multiple diseases), using sequential enzymatic digestion and dissociation, Optiprep density gradient to remove large debris, followed by magnetic activated cell sorting (MACS) (**Supplementary Figure 1a**). CPCs were magnetically enriched based upon a CD45-negative, CD31-negative, CD34-negative, and c-

kit-positive sorting strategy (Smith et al. 2014; Vicinanza et al. 2017) (**Supplementary Figure 1b**). Despite being recognised as a CPC marker, cells were not sorted for Sca-1 because its homology has not been confirmed in any species other than mouse. By flow cytometry analysis, CPCs showed expression of other recognised CPC markers such as CD90 (37±0.4%), CD166 (41±1%), CD105 (13±1%), and CD140α (5±0.4%) (**Supplementary Figure 1c**). There were no differences in number of CPCs isolated from old (>70 years) subjects, compared to subjects <70 years. We also found no differences in number of CPCs isolated from male or female, or from those subjects with valve disease, coronary disease or aortic disease (**Supplementary Figure 1d).**

We isolated CPCs from 35 subjects of different genders, ages, and pathologies and found a linear increase (R^2=0.722) in the number of freshly isolated CPCs that expressed the senescence-associated marker, $p16^{INK4A}$, with age (**Figure 1a**). Although a trend was evident, n~~N~~o differences were evident between males and females for $p16^{INK4A}$ expression or between aortic disease, valvular disease, coronary artery disease, and multiple other diseases for $p16^{INK4A}$ expression (**Supplementary Figure 2a,b**). Moreover, we found no differences between smokers (including ex-smokers) and non-smokers, diabetics and non-diabetics, and hypertensive and non-hypertensive subjects for $p16^{INK4A}$-expressing CPCs (**Supplementary Figure 2c-e)**. On average, 22±9%, 31±4%, 48±9%, and 56±16% of freshly isolated CPCs expressed $p16^{INK4A}$~~nk4a~~ isolated from 50-59, 60-69, 70-79, and 80-89 year old subjects, respectively (**Figure 1a**). We also found an increase ($P<0.05$) in the number of senescence-associated β-galactosidase- (SA-β-gal; ~60%) and DNA damage marker, γH2AX-positive CPCs (~20%) freshly isolated from old (71-79 years), compared to middle-aged (54-63 years) subjects (**Figure 1b,c**). Moreover, $p16^{INK4A}$-positive CPCs co-expressed γH2AX (**Figure 1c**). Further interrogation by Q-FISH revealed that, while the average telomere length of CPCs freshly isolated from old and middle-aged subjects' hearts were comparable, CPCs freshly isolated from old (78-84 years) subjects' hearts contained a 12% subpopulation with telomere length of <6Kb, which is regarded as being critically short (**Figure 1d**) (Canela et al. 2007). Approximately 2% of the CPCs freshly isolated from human hearts were Ki67-positive, reflective of their mainly dormant, quiescent phenotype (Ellison et al. 2013). There were no differences between middle-aged and old subjects in number of Ki67-positive CPCs, and we did not see any Ki67-positive CPCs that were $p16^{INK4A}$-positive (**Supplementary Figure 2f**~~e~~). These findings indicate that the aged human heart contains an increased proportion of aged senescent-CPCs, which could translate to their dysfunctionality.

Formatted: Superscript

Formatted: Font: Bold

CPCs from old subjects show impaired cell growth and differentiation

CPCs were isolated from 5 old (76-86 years) and 8 middle-aged (32-66 years) subjects, plated in growth medium, and propagated, where possible, to passage 11. CPCs isolated from 2 of the middle-aged (32 and 61 years) and ~~3~~ 2 of the oldest (78 and~~,~~ 80~~, and 86~~ years) subjects failed to grow and become established *in vitro*. ~~.~~ Of the CPC cultures that did grow from all age groups (n=8), the CPCs, from P3 to P11, gradually lost their $p16^{INK4A}$–positive subpopulation (**Supplementary Figure 2g~~d,e~~**), likely due to the cell culture activated, cycling-competent CPCs outgrowing their $p16^{INK4A}$–positive senescent counterparts. CPCs maintained the phenotype of c-kit-positive, CD31-negative over culture passage (**Supplementary Figure 2h~~f~~**). To ensure that the effect of donor age could be effectively evaluated, all *in vitro* cell dynamic assays were performed between P2-P4.

CPCs isolated from old (77-86 years) subjects showed decreased ($P<0.05$) proliferation compared to CPCs isolated from middle-aged (34-62 years) subjects (**Figure 2a**). CPCs deposited as a single-cell in a 96-well plate generated a greater number ($P<0.05$) of clones if the single CPCs originated from middle-aged (34-62 years) subjects, compared to old (76-86 years) subjects (**Figure 2b**). Likewise, CPCs deposited at low dilution in bacteriological dishes for the generation of spheres in suspension were greater in number and size ($P<0.05$) for middle-aged (34-51 years) subject~~'~~s' CPCs, compared to old (76-77 years) subject~~'~~s' CPCs (**Figure 2c,d**). When CPCs were plated in cardiomyocyte differentiation medium, they primed towards a cardiomyocyte-like precursor cell type that was Nkx2.5-positive, sarcomeric actin-positive, and m~~M~~iddle-aged (47-62 years) subject's CPCs had increased ($P<0.05$) differentiation potential, compared to CPCs from old (76-77 years) subjects (**Figure 2e-g**). Older subject's differentiated CPC-derived precursor cells showed disorganised sarcomeric structure (**Figure 2e**) and decreased ($P<0.05$) expression (**Figure 2g**), compared to differentiated CPCs from younger, middle-aged subjects.

Even though CPCs isolated from old hearts showed decreased proliferation, clonogenicity, and differentiation potential, only ~50% of CPCs are senescent in old myocardium (**Figure 1a**), therefore these data imply that a functionally cycling-competent CPC population still exists in old myocardium. Indeed, single CPC-derived clones from younger ~~young, middle-aged,~~ and old subjects were indistinguishable in terms of morphology, senescence, multipotency, self-renewing transcript profile, and differentiation (**Supplementary Figure**

3). These findings suggest that CPCs age and become senescent in a stochastic, non-autonomous manner. This resembles what was seen in rat preadipocytes (Kirkland et al. 1990).

Aged-senescent CPCs lose their regenerative capacity *in vivo*

To purify for a senescent population of CPCs we utilised the C_{12}-5-Dodecanoylaminofluorescein Di- β -D-Galactopyranoside (C12FDG) probe and pulled out SA-β-gal-positive CPCs through FACS (**Supplementary Figure 4a-d**). We also induced senescence in CPCs pharmacologically using Doxorubicin and Rosiglitazone (**Supplementary Figure 4e-g**), which we have used previously to render cells to senescence *in vitro* (Xu et al. 2015 ~~eLIFE~~; Xu et al. 2018). Senescent-CPCs, whether Doxorubicin-, or Rosiglitazone-induced or purified using the C12FDG probe, exhibited a senescent phenotype being $p16^{INK4A}$–positive, Ki67-negative, and with shorter telomeres (**Supplementary Figure 5**). Senescent SA-β-gal-positive CPCs were non-proliferative and did not form clonal colonies when deposited as single cells, or generate spheres *in vitro*, compared to SA-β-gal-negative, Ki67-positive cycling-competent CPCs (**Supplementary Figure 5**). FACS phenotyping revealed decreased surface expression of the progenitor markers, c-kit, CD90, CD105, and CD166 and increased expression of CD31 and CD34 in SA-β-gal-positive, senescent-CPCs compared to SA-β-gal-negative, cycling-competent CPCs (**Supplementary Figure 6**).

To determine whether the dysfunctional stem/progenitor cell properties of the senescent-CPCs translated *in vivo*, we tested the regenerative capacity of doxorubicin-induced senescent SA-β-gal-positive CPCs and cycling-competent SA-β-gal-negative CPCs in the myocardial infarction-regeneration mouse model (**Figure 3a**). To separate the impact of senescence from other potentially confounding aging processes operative in older mice, such as NAD deficiency, accumulation of advanced glycation end products, or accumulation of misfolded proteins, we transplanted senescent or and cycling-competent CPCs into young mice. Male, immunodeficient NSG mice were subjected to permanent ligation of the left anterior descending (LAD) coronary artery. Immediately after ligation, 5 x 10^5 SA-β-gal-positive senescent or SA-β-gal-negative cycling-competent CPCs were injected intramyocardially in 15µl of PBS at 2 sites in the border zone. To serve as a cell control, a separate set of MI-mice were injected with 5 x 10^5 non-CPCs (c-kit^{neg} cardiac-derived cells; containing 86±5%

cardiac fibroblasts, 13±3% vascular smooth muscle, 1±1% endothelial cells (Ellison et al. 2013)). Sham animals were treated the same way, except ligation of LAD coronary artery was not performed and they did not receive cells but were injected with the same volume of PBS. Mice were administered BrdU *via* osmotic mini pumps for 14 days after MI and cell injection to track new cell DNA formation (**Figure 3a**). All cell populations were labelled prior to injection with PKH26 lipophilic membrane dye, which exhibited high labelling efficiency and label dye retention over population doublings in cycling-competent CPCs and c-kit^{neg} cardiac-derived cells *in vitro* (**Supplementary Figure 7**). We sacrificed a sub-set of MI-mice that had been injected with 5 x 10^5 SA-β-gal-negative cycling-competent CPCs at 4 days. There was high engraftment and survival of CPCs within the infarct/border zone at 4 days (**Figure 3b**) and by 28 days the engraftment was still ~10% of cycling-competent CPCs per total nuclei in the infarct/border zone (**Figure 3c**). The engraftment and survival of senescent-CPCs and c-kit^{neg} cells at 28 days was significantly ($P<0.05$) less (**Figure 3c**).

At 1 week after LAD ligation all groups had decreased ($P<0.05$) LV function, compared to baseline and sham controls, however the group that had been injected with cycling-competent CPCs had less of a decrease in LV function at 1 week, compared to the senescent-CPC and non-CPC c-kit^{neg} cell groups (**Figure 3d**). The degree of MI represented as the % Average Area at Risk (AAR) through Evans Blue staining immediately after MI was 33.0±1.6% (n=5), demonstrating the operator as being extremely consistent in inducing a similar size MI injury to each mouse. At 4 weeks after LAD ligation, MI hearts that had received cycling-competent CPCs showed an improvement ($P<0.05$) in LV ejection fraction (EF), fractional shortening (FS), LVEDD, and LVESD, which had almost returned to baseline values and to that of Sham controls (**Figure 3d**).

This extent of LV improvement was not apparent in MI-mice that were injected with SA-β-gal-positive senescent-CPCs, or the non-CPC c-kit^{neg} cell group that showed no recovery with worsened LV function and were all in heart failure at 4 weeks (**Figure 3d**). To accompany these functional changes, cycling-competent CPC injection resulted in a decreased ($P<0.05$) infarct size, whereas SA-β-gal-positive senescent-CPCs or non-CPC c-kit^{neg} cells did not change the extent of infarct size (**Figure 3e**). Immunohistochemical analysis of cross-sections revealed that at 4 weeks after MI, the transplanted PKH26-labelled cycling-competent CPCs had increased expression of sarcomeric proteins, α-actinin, as well as the endothelial lineage marker vWF, evidencing their differentiation into cardiomyocyte-like precursor cells and

endothelial cells, respectively (**Figure 3f; Supplementary Figure 8a,b**). Limited or no differentiation was evident in the infarcted/border zone of the hearts injected with PKH26-labelled senescent-CPCs and non-CPC c-kit^{neg} cells (**Figure 3f**). To determine whether the transplanted cells had participated in inducing a paracrine effect, the infarct/border zone of hearts that had received cells were analysed for formation of new cells that were BrdU-positive/PKH26-negative. Hearts that were injected with cycling-competent CPCs showed an increased number of BrdU-positive cells, compared to those injected with SA-β-gal-positive senescent-CPCs or non-CPC c-kit^{neg} cells (**Supplementary Figure 8c,d**). Moreover, these BrdU-positive cells co-localised with vWF or α-sarcomeric actinin, indicating ~~new~~ that these endothelial (capillary) cells and cardiomyocytes had been prompted to initiate DNA synthesis and suggest they may have entered the cell cycle~~formation, respectively~~. ~~New~~ BrdU-positive cardiomyocyte and capillaries~~ry formation~~ were~~as~~ more evident ($P<0.05$) in the MI-cycling-competent CPC group (**Figure 3g**). These findings show the diminished regenerative and reparative capacity of senescent CPCs, compared to healthy, cycling-competent CPCs.

Aged-Senescent CPCs have a Senescence-Associated Secretory Phenotype (SASP)

Senescent cells exhibit a SASP (Tchkonia et al. 2013). Senescent SA-β-gal-positive CPCs showed increased expression of SASP factors, including MMP-3, PAI1, IL-6, IL-8, IL-1β, and GM-CSF, compared to non-senescent, SA-β-gal-negative, cycling-competent CPCs (**Figure 4a**). To determine whether the SASP factors were secreted from senescent-CPCs, we quantified the protein levels of seven of the highly expressed SASP factors in conditioned media from senescent-CPCs using Luminex technology. We found increased ($P<0.05$) quantities of all seven SASP factors in senescent-CPC conditioned medium, compared to conditioned medium of cycling-competent CPCs (**Figure 4b**). Next we treated cycling-competent CPCs with conditioned medium from senescent-CPCs and measured cell proliferation and senescence of the cycling-competent CPCs. Conditioned medium from senescent-CPCs resulted in decreased ($P<0.05$) proliferation (**Figure 4c**) and an increased ($P<0.05$) proportion of senescent p16^{INK4A}–positive, SA-β-gal-positive, and γH2AX-positive CPCs in the culture, compared to CPCs treated with conditioned medium from cycling-competent CPCs or unconditioned medium (**Figure 4d-f**). These findings show that the senescent-CPCs exhibit a SASP, which can negatively impact surrounding cells, rendering otherwise healthy, cycling-competent CPCs to lose proliferative capacity and switch to a senescent phenotype. This is consistent with the spread of senescence to recipients' cells that

we observed after transplanting another senescent progenitor cell type, senescent adipocyte progenitors (Xu et al. 2018).

Elimination of senescent CPCs using senolytic drugs abrogates the SASP *in vitro*

Removal of $p16^{Ink4a}$ senescent cells can delay the acquisition of age-related pathologies in adipose tissue, skeletal muscle, heart, blood vessels, lung, liver, bone, and eye (Baker et al. 2011; Xu et al. 2015; Roos et al. 2016; Farr et al. 2017; Ogrodnik et al. 2017; Schafer et al. 2017; Xu et al. 2018, Zhu et al. 2015; Lehmann et al. 2017; Baker et al. 2016). Recent studies have documented the use of senolytic drugs for the selective clearance of senescent cells from 'aged' tissues (Tchkonia and Kirkland, 2018). We tested the potential of 4 senolytic drugs, Dasatinib (D; an FDA-approved tyrosine kinase inhibitor), Quercetin (Q; a flavonoid present in many fruits and vegetables), Fisetin (F; also a flavonoid), and Navitoclax (N; an inhibitor of several BCL-2 family proteins), alone and in combination to eliminate and clear senescent-CPCs *in vitro* (**Supplementary Figure 9a**). Measuring cell viability with crystal violet and number of SA-β-gal-positive CPCs, dose-response experiments on senescent- or cycling-competent CPCs from the same subjects showed D and N to effectively clear senescent-CPCs, whereas F and Q were less effective at clearing senescent-CPCs (**Supplementary Figure 9b,c**). However, D also decreased the viability of cycling-competent CPCs (**Supplementary Figure 9b**). A combination of D+Q, which has previously shown to yield effective senescent cell clearance (Roos et al. 2016; Farr et al. 2017; Ogrodnik et al. 2017; Schafer et al. 2017; Xu et al. 2018, Zhu et al. 2015; Lehmann et al. 2017) and which does not share the toxic anti-neutrophil and anti-platelet side effects of N (Kirkland et al. 2015; Kirkland and Tchkonia, 2017) was tested, and at a dose of 0.5μM D with 20μM Q, cycling-competent CPC viability was preserved (**Figure 5a**), but senescent-CPCs were cleared and induced to selective apoptosis (**Supplementary Figure 9d**).

We next determined whether clearing senescent-CPCs using D+Q would abrogate the SASP and its paracrine impact on CPCs. Using transwell inserts, cycling-competent CPCs were seeded on the top chamber insert and co-cultured in the presence of senescent-CPCs seeded on the bottom chamber. Cultures were left for 7 days and then cycling-competent CPCs in the top chamber were analysed for proliferation and markers of senescence, $p16^{INK4A}$, SA-β-gal, and γH2AX, and conditioned medium analysed for SASP factors. The cultures were then treated with D+Q for 3 days to clear the senescent-CPCs on the bottom chamber, and then 7 days later cycling-competent CPCs in the top chamber were analysed for proliferation and the

markers of senescence, $p16^{INK4A}$, SA-β-gal, and γH2AX, and conditioned medium analysed for SASP factors (total of 17 days; **Supplementary Figure 9a**). We found that cycling-competent CPCs co-cultured in the presence of senescent-CPCs for 7 days were decreased ($P<0.05$) in number and proliferation, and had increased ($P<0.05$) expression of $p16^{INK4A}$, SA-β-gal, and γH2AX (**Figure 5b-f**). Application of D+Q to co-cultures eliminated the senescent-CPCs (**Figure 5g**) and 7 days later, the cycling-competent CPCs had increased ($P<0.05$) in number (**Figure 5h**), proliferation (**Figure 5i**), and the number of $p16^{INK4A}$ and SA-β-gal CPCs had decreased ($P<0.05$) compared to CPCs that had been in co-culture with senescent-CPCs for 17 days (**Figure 5j,k**). Co-culture of cycling-competent CPCs with senescent-CPCs led to increased ($P<0.05$) secretion of SASP factors into the medium, but the level of SASP factors was reduced ($P<0.05$) with application of D+Q (**Figure 5l**). These findings document that senescent CPCs have a SASP, and clearance of senescent CPCs using a combination of D+Q senolytics abrogates the SASP and its detrimental senescence-inducing effect on healthy, cycling-competent CPCs.

Elimination of senescent cells *in vivo* activates resident CPCs and increases number of small, proliferating cardiomyocytes in the aged heart

To determine the effects of global senescent cell removal on the heart, 24-32 month INK-ATTAC transgenic or wild-type mice were randomised to either vehicle, AP20187, or D+Q treatment, administered in 4 cycles for 3 consecutive days/cycle, 12 days apart. Mice were sacrificed 4 days after the last dose of cycle 4 (**Figure 6a**). Tissues in which $p16^{Ink4a}$ expression and/or senescent cells are decreased by D+Q in wild type mice as well as by AP20187 in INK-ATTAC mice include the aorta, adipose tissue, cardiac and skeletal muscle, lung, liver, and bone (Baker et al. 2016; Roos et al. 2016; Farr et al. 2017; Ogrodnik et al. 2017; Schafer et al. 2017; Xu et al. 2018, Zhu et al. 2015; Lehmann et al. 2017).We showed $p16^{Ink4a}$ mRNA expression was decreased ($P<0.05$) in the heart following D+Q or AP20187 treatment in aged INK-ATTAC or wildtype mice (**Figure 6b**).

Previously we have shown an improvement of heart function in old mice after D+Q treatment (Zhu et al. 2015). Analysis of cardiac cross-sections revealed significantly higher ($P<0.05$) CPC ($Sca\text{-}1^{+}/c\text{-}kit^{+}/CD45^{-}/CD31^{-}/CD34^{-}$) ~~(Vicinanza et al. 2017)~~ numbers (**Figure 6c; Supplementary Figure 10a**) in AP20187-treated INK-ATTAC mice and D+Q-treated INK-ATTAC or wild-type mice, compared to vehicle-treated control. Interestingly, D+Q treatment showed increased ($P<0.05$) CPC number, compared to AP20187-treatment (**Figure 6c**).

Roughly 10% of CPCs were activated and in the cell cycle (Ki67-positive) at the time of sacrifice, after AP20187 or D+Q treatment (**Supplementary Figure 10b**). Morphometric analysis of heart sections showed that AP20187-treated and D+Q-treated mice had increased number of smaller ventricular myocytes (**Figure 6d**), suggesting these myocytes to be immature and newly formed, compared to vehicle-treated mice, which exhibited only rare small myocytes but a greater proportion of hypertrophied myocytes (**Figure 6d**). We found an increase ($P<0.05$) of small, proliferating Ki67-positive myocytes (~0.25%) in old hearts following AP20187- or D+Q-treatment, compared to vehicle-treated control (0.03±0.03%) (**Figure 6e,f**). To corroborate these data we injected EdU 4 days and 2 hours prior to sacrifice of old (22m) and young (3m) AP20187-treated INK-ATTAC mice (**Supplementary Figure 10c**). We found increased ($P<0.05$) number of small EdU-positive myocytes (0.25±0.06%; **Figure 6g,h**) in the hearts of old AP-treated mice, compared to old vehicle-treated (0.07±0.00%), young vehicle-treated (0.12±0.03%) and young AP-treated (0.11±0.04%) mice. The number of EdU-positive myocytes in the old AP-treated INK-ATTAC mice was the same in amount to Ki67-positive myocytes (~0.25%) in AP20187- or D+Q-treated mouse hearts (**Figure 6f**). Finally, we detected a decrease ($P<0.05$) in fibrosis in the LV following AP20187- and D+Q-treatment, compared to vehicle-treated control (**Figure 6i**). In contrast to the treatment of aged mice, treatment of young adult (2-3 Months) INK-ATTAC or wild-type mice with AP20187 or D+Q, respectively, did not alter EdU-positive myocyte number (**Figure 6h**), CPC numbers or myocyte diameter (*data not shown*). These findings show that clearance of senescent cells leads to stimulation of CPCs and cardiomyocytes with increased DNA-synthesising activity ~~proliferation~~ and that this strategy is specific to the aged heart.

Discussion

~~In a large sample cohort~~ Our study shows that CPCs isolated from the failing human heart develop a senescent phenotype with age exhibited by increased expression of senescence-associated markers ($p16^{INK4A}$, SA-β-gal), DNA damage, shortened telomere length and a SASP. Aged human hearts with dilated cardiomyopathy showed greater numbers of $p16^{INK4A}$ –positive CPCs and cardiomyocytes with shorter telomeres than age-matched controls (Chimenti et al. 2003). Similarly, CPCs isolated from failing, aged hearts show increased $p16^{INK4A}$ and inflammatory factor expression (Cesselli et al. 2011). Reliably detecting senescent cells *in vivo* is an ongoing challenge, and it is important that a combination of senescent cell biomarkers are used for detection as any one marker used in isolation is prone to false positives. Our study used a combined panel of the senescence-associated biomarkers,

Formatted: Font: Italic

p16^{INK4A}, γH2AX, telomere length, SA β-gal activity and SASP expression, to detect senescent CPCs. A limitation of our study is that because of low yield of CPCs isolated from small myocardial samples (~45,000 per gram of tissue) we were unable to evaluate the expression of SASP factors on freshly isolated CPCs, or test the effects of the SASP of freshly isolated CPCs *in vitro*. Our findings demonstrate that CPCs accumulate in the failing hearts of elderly subjects (>76 years) and are dysfunctional, showing impaired proliferation, clonogenicity, spherogenesis, and differentiation, compared to CPCs isolated from the hearts of middle-aged (32-66 years) subjects. As the adult heart possesses very low numbers (<1% of c-kit^{pos} cells) of cardiomyogenic CPCs (Vicinanza et al. 2017), if by 80 years of age >50% of resident CPCs are senescent, this presents a bleak outcome for harvesting healthy, functional CPCs from patients who are candidates for regenerative therapies and their autologous use. Moreover, strategies to activate the regenerative capacity of the aged heart through delivery of growth factors or cell therapy will also be sub-optimal. Therefore, the success of cardiac regenerative therapeutic approaches thus far tested for treating patients with heart failure and disease could be of limited efficacy in promoting myocardial regeneration because of the increased number of senescent, dysfunctional CPCs and cardiomyocytes (Chimenti et al. 2003; Cesselli et al. 2011) and the resultant presence of a cardiac SASP in the aged and failing heart that impairs the function of the remaining non-senescent CPCs. These findings may also have implications regarding the use hearts from aged *vs*. younger donors for transplantation (Lau et al. 2019).

The present study found that CPCs age in a stochastic non-autonomous manner and it is possible to clonally select from a single CPC for a cycling-competent population of CPCs even from diseased or aged hearts. There are individual CPCs in older individuals that have replicative and functional capacities resembling those of CPCs in younger subjects. A similar scenario was found in the case of rat fat cell progenitors (Kirkland et al. 1990). While the abundance of progenitors cloned from adipose tissue that had restricted capacities for replication and differentiation into adipocytes or that were non-replicative but viable (*i.e.*, senescent) increased progressively with aging in rat fat, there remained cells that had the capacities for replication and adipogenic differentiation characteristic of clones derived from young rats. In the present study we utilised hypoxic conditions (5% CO_2, 2% O_2) to expand viable CPCs. Other interventional approaches have shown that senescence characteristics of human CPCs are alleviated by Pim-1 kinase resulting in rejuvenation of CPC phenotypic and functional properties (Mohsin et al. 2013). Together, these findings indicate that: (1) it may

Formatted: Font: Italic

Formatted: Not Highlight

be feasible to isolate and propagate CPCs even from older individuals that are functional, capable of supporting cardiac regeneration if removed from their toxic *milieu*, and that could be therapeutically relevant in treating patients, especially if they were autologously generated and (2) that by clearing senescent CPCs with a toxic SASP from the aged heart, there remains a tissue-resident population of CPCs with regenerative and reparative potential.

When we purified for a homogenous SA-β-gal-positive, senescent CPC population, we showed that these cells had poor engraftment and survival, and were unable to contribute to cardiac regeneration, repair or restoration of cardiac function following transplantation into the infarcted myocardium. This is contrary to *in vitro*-selected, SA-β-gal-negative, proliferative cycling-competent ($Ki67^{pos}$) CPCs, which had high survival and engraftment in the infarct/border zone, restored cardiac function almost to baseline and sham control values (LVEF 59±2% at 28 days vs. 66±2 at baseline), decreased infarct size, differentiated into endothelial and cardiomyocyte-like precursor cells as well as enhanced endogenous ~~new~~ $BrdU^{pos}$ cardiomyocyte and capillaries.~~y formation.~~ Although some of the transplanted CPCs expressed α-sarcomeric actin, these cells did not exhibit the typical cardiomyocyte phenotype as they were small and lacked a structured sarcomeric unit. Therefore, they could not be considered as new, immature myocytes ~~which~~ that contributed physiologically to the substantially improved LV function. There is now a general consensus that the favourable effect of cell transplantation protocols is, at least in part, mediated by 'paracrine' effectors secreted by the transplanted cells, contributing to improved myocardial contractility and amelioration of ventricular remodelling (decreasing fibrosis, hibernation, and stunning), inhibition of the inflammatory response, and increased cardiomyocyte survival, cardiomyogenesis and angiogenesis/neovascularisation (Broughton et al. 2018). The present data emphasize the importance of taking into account the hostile infarcted environment, which does not favour engraftment, differentiation or maturation of newly formed cardiomyocytes derived from injected cells. However, the presence of CPC-derived cardiomyocyte precursors expressing sarcomeric protein in the infarct/border zone is promising and further work should elucidate how to mature these cells into functionally competent contractile cells.

Like the present study, not all experimental studies have shown physiological regeneration of CPC-derived cardiac muscle following administration of CPCs (Tang et al. 2016). This is most likely due to the heterogeneous nature of cardiac c-kit positive cells tested, with only a

very small fraction (1-2%) having properties of stem cells (Vicinanza et al. 2017). Bringing together the cardiomyogenic potential of CPCs, which can be amplified in number through *in vitro* single cell-derived clonal selection and CPC-mediated cytokine release, advocate CPCs as an ideal candidate for cardiac regenerative interventions.

Senescent cells have emerged as bona fide drivers of aging and age-related CVD, which suggests strategies aimed at reducing or eliminating senescent cells could be a viable target to treat and prevent CVD (Childs et al. 2018). In 18 month old INK-ATTAC mice $p16^{INK4a}$-positive cells contribute to cardiac aging and these senescent cells decreased following AP20187-treatment (Baker et al. 2016). Moreover, D+Q administration over 3 months decreased senescent cell markers (TAF+ cells) in the media layer of the aorta from aged (24 months) and hypercholesterolemic mice, which was met with improved vasomotor function (Roos et al. 2016). We show for the first time that the genetic and pharmacological approaches used here to reduce senescent cell burden leads to increased number of CPCs and smaller ventricular myocytes, which were Ki67-positive and EdU-positive, suggesting these myocytes to be immature and newly formed (Ellison et al. 2013), compared to vehicle-treated mice, which exhibited very rare small myocytes but a greater proportion of hypertrophied myocytes. These findings are in line with those of Baker et al. (2016) who showed that AP-treated INK-ATTAC mice had smaller ventricular cardiomyocytes.

The frequency of resident cardiac stem and progenitor cells in the healthy myocardium of several mammalian species, including human, mouse, rat, and pig, is approximately one per every 1000–2000 myocytes, depending on age (Torella et al. 2007). We detected a 16- and 23-fold increase in the number of CPCs following elimination of senescent cells by AP- or D+Q-treatment in the aged mouse heart, respectively. Moreover, ~10% of CPCs after elimination of senescent cells were activated, expressing Ki67. The number of Ki67-positive and EdU-positive cardiomyocytes increased 9- and 4-fold in the aged heart, respectively, following clearance of senescent cells by either D+Q- or AP-treatment. We show that t~~T~~he number of ~~proliferating~~ DNA-synthesising cardiomyocytes present in the young (3 month old) mouse heart is 0.12±0.03% of total cardiomyocytes, and the number of DNA-synthesising ~~proliferating~~ cardiomyocytes present in the old (22 month old) mouse heart is 0.07±0.00% of total cardiomyocytes. Elimination of senescent cells lead to double the amount of the proliferating cardiomyocytes found in a young heart, and triple the number found in an old heart. Therefore, the present data represent a significant and physiologically

relevant increase and activation of the resident CPC compartment and increased cardiomyocyte ~~proliferation~~ DNA synthetic activity following clearance of senescent cells. These findings are consistent with the hypothesis that clearing senescent cells can beneficially alter stem and progenitor cell function across multiple tissues. D+Q enhances function of osteoblastic progenitors, leading to new bone formation in mice with age-related osteoporosis, impedes function of the osteoclast progenitors that lead to bone resorption in these same mice (Farr et al. 2017), and enhances neurogenesis in mice with metabolically-induced impairment of nerve cell generation (Ogrodnik et al. 2018).

Formatted: Not Highlight

Previous work has shown that senescent human primary preadipocytes, human omental adipose tissue cells obtained from obese individuals (45.7±8.3 years), as well as human umbilical vein endothelial cells (HUVECs) develop a SASP with aging, which induced inflammation in healthy adipose tissue and preadipocytes (Xu et al. 2018; , Xu et al. 2015). Clearance of senescent cells using D+Q decreased the secretion of key SASP components, PAI-1, GM-CSF, IL-6, IL-8 and MCP-1 (Xu et al. 2018). In the present study, clearance of senescent human CPCs using D+Q abrogated the SASP, and the deleterious impact of the SASP on CPC proliferation and inducing senescence. Thus D+Q can kill human senescent cells, including tissue specific stem/progenitor cells, and can attenuate the secretion of inflammatory cytokines associated with human age-related frailty (Xu et al. 2018). Consistent with this, in the first human trial of senolytics, subjects with idiopathic pulmonary fibrosis had enhanced walking endurance, gait speed, chair rise test performance, and scores in the Short Physical Performance Battery 5 days after 9 doses of D+Q over 3 weeks (Justice et al. 2018).

In conclusion, the present work, albeit performed in mice models, demonstrates approaches that eliminate senescent cells may be useful for treating age-related cardiac deterioration and rejuvenating the regenerative capacity of the aged heart. However, caution should be exercised in interpreting mouse data considering previous cardiac regenerative strategies where bone marrow derived cells were injected into mouse MI models did not translate into equivalent outcomes in humans. Future work should address the effects of senolytic agents on improving cardiac function and alleviating the SASP, resulting in an improved microenvironment in vivo and the activity of other cell types such as fibroblasts and endothelial cells. Indeed, ~~The~~ next steps ~~would be to~~should determine whether senolytic approaches could be used in conjunction with cell therapy interventions to improve the

environment (the 'soil') that the cells (the 'seeds') are ~~being~~ transplanted into and therefore ameliorate intrinsic reparative mechanistic processes that are compromised with age (Lau et al. 2019). Indeed, targeting senescent cells could also impact the potency of resident stem/progenitor populations in other aged organs. The present findings provide new insights into therapies that target senescent cells to prevent an age-related loss of regenerative capacity.

Experimental Procedures

Expanded experimental procedures are in the supporting information.

Myocardial samples (~200mg each) were obtained from the right atrial appendage (total samples, n=119) of human subjects with cardiovascular disease, aged 32-86 years. Subjects aged 70-86 years were included in the old group. Subjects aged 32-67 years were included in the middle-aged group. All subjects gave informed consent before taking part in the study (NREC #08/ H1306/91). Cardiac tissue was minced and enzymatically digested to release cardiac small cells. CPCs were purified by first depleting $CD45^{pos}$ and $CD31^{pos}$ cells by immunolabelling with anti-human CD45 and CD31 magnetic immunobeads (Miltenyi), and then the CD45- CD31-depleted fraction was enriched for $c\text{-}kit^{pos}$ cells through incubation with anti-human CD117 immunobeads (Miltenyi). CPCs were characterised by flow cytometry for other CPC markers before proceeding with functional *in vitro* and *in vivo* assays. All animal surgical experiments were conducted in accordance with the regulations of the Home Office and stipulated under the Animals (Scientific Procedures) Act 1986.

Acknowledgements: We acknowledge Thomas Theologou and Mark Field from Liverpool Heart & Chest Hospital, Liverpool, UK for ~~giving~~ providing some myocardial samples. Carl Hobbs (KCL) for tissue processing, histology, and microscopic analysis assistance. Confocal microscopy was carried out in the Nikon Imaging Centre, KCL. This work was supported by British Heart Foundation project grant PG/14/11/30657 (GME-H and J.E.C.), NIH grant AG13925 (JLK), the Connor Group (JLK), Robert J. and Theresa W. Ryan (JLK), Robert and Arlene Kogod (JLK), the Noaber Foundation (JLK), and a Glenn/American Federation for Aging Research (AFAR) BIG Award (J.L.K.).

Author contributions: F.C.L-M., P.J.R., E.D-V., T.S.T., B.J.C., and L.P performed experiments and analysis. J.E.C., and D.T were involved in conceptualisation. F.C.L-M., P.J.R., T.T., G.M.E-H., and J.L.K were involved in conceptualisation, writing, and editing. G.M.E-H., T.T., and J.L.K supervised and performed funding acquisition.

References

Baker, D. J., Childs, B. G., Durik, M., Wijers, M. E., Sieben, C. J., Zhong, J., . . . van Deursen, J. M. (2016). Naturally occurring p16Ink4a-positive cells shorten healthy lifespan. *Nature, 530*(7589), 184-189. doi:10.1038/nature16932

Baker, D. J., Wijshake, T., Tchkonia, T., LeBrasseur, N. K., Childs, B. G., van de Sluis, B., . . . van Deursen, J. M. (2011). Clearance of p16Ink4a-positive senescent cells delays ageing-associated disorders. *Nature, 479*, 232. doi:10.1038/nature10600

Bergmann, O., Bhardwaj, R. D., Bernard, S., Zdunek, S., Barnabe-Heider, F., Walsh, S., . . . Frisen, J. (2009). Evidence for cardiomyocyte renewal in humans. *Science, 324*(5923), 98-102. doi:10.1126/science.1164680

Broughton, K. M., Wang, B. J., Firouzi, F., Khalafalla, F., Dimmeler, S., Fernandez-Aviles, F., & Sussman, M. A. (2018). Mechanisms of Cardiac Repair and Regeneration. *Circ Res, 122*(8), 1151-1163. doi:10.1161/circresaha.117.312586

Canela, A., Vera, E., Klatt, P., & Blasco, M. A. (2007). High-throughput telomere length quantification by FISH and its application to human population studies. *Proceedings of the National Academy of Sciences, 104*(13), 5300-5305. doi:10.1073/pnas.0609367104

Castaldi, A., Dodia, R. M., Orogo, A. M., Zambrano, C. M., Najor, R. H., Gustafsson, A. B., . . . Purcell, N. H. (2017). Decline in cellular function of aged mouse c-kit(+) cardiac progenitor cells. *J Physiol, 595*(19), 6249-6262. doi:10.1113/jp274775

Cesselli, D., Beltrami, A. P., D'Aurizio, F., Marcon, P., Bergamin, N., Toffoletto, B., . . . Leri, A. (2011). Effects of Age and Heart Failure on Human Cardiac Stem Cell Function. *The American Journal of Pathology, 179*(1), 349-366. doi:https://doi.org/10.1016/j.ajpath.2011.03.036

Childs, B. G., Li, H., & van Deursen, J. M. (2018). Senescent cells: a therapeutic target for cardiovascular disease. *The Journal of Clinical Investigation, 128*(4), 1217-1228. doi:10.1172/JCI95146

Chimenti, C., Kajstura, J., Torella, D., Urbanek, K., Heleniak, H., Colussi, C., . . . Anversa, P. (2003). Senescence and Death of Primitive Cells and Myocytes Lead to Premature Cardiac Aging and Heart Failure. *Circulation Research, 93*(7), 604.

Ellison-Hughes, G. M., & Lewis, F. C. (2017). Progenitor Cells from the Adult Heart. In M. Ieda & W.-H. Zimmermann (Eds.), *Cardiac Regeneration* (pp. 19-39). Cham: Springer International Publishing.

.

Ellison, G M., Vicinanza, C., Smith, Andrew J., Aquila, I., Leone, A., Waring, Cheryl D., . . . Nadal-Ginard, B. (2013). Adult c-kitpos Cardiac Stem Cells Are Necessary and Sufficient for Functional Cardiac Regeneration and Repair. *Cell, 154*(4), 827-842. doi:https://doi.org/10.1016/j.cell.2013.07.039

Farr, J. N., Xu, M., Weivoda, M. M., Monroe, D. G., Fraser, D. G., Onken, J. L., . . . Khosla, S. (2017). Targeting cellular senescence prevents age-related bone loss in mice. *Nat Med, 23*(9), 1072-1079. doi:10.1038/nm.4385

Herbig, U., Ferreira, M., Condel, L., Carey, D., & Sedivy, J. M. (2006). Cellular Senescence in Aging Primates. *Science, 311*(5765), 1257. doi:10.1126/science.1122446

Hsieh, P. C., Segers, V. F., Davis, M. E., MacGillivray, C., Gannon, J., Molkentin, J. D., . . . Lee, R. T. (2007). Evidence from a genetic fate-mapping study that stem cells refresh adult mammalian cardiomyocytes after injury. *Nat Med, 13*(8), 970-974. doi:10.1038/nm1618

Jeyapalan, J. C., & Sedivy, J. M. (2008). Cellular senescence and organismal aging. *Mechanisms of Ageing and Development, 129*(7), 467-474. doi:https://doi.org/10.1016/j.mad.2008.04.001

Justice, J.N., Nambiar, A.M., Tchkonia, T., LeBrasseur, N.K., Pascual, R., Hashmi, S.K., Prata, L., Masternak, M.M., Kritchevsky, S.B., Musi, N., Kirkland, J.L. Senolytics in

idiopathic pulmonary fibrosis: results from a first-in-human, open-label, pilot study. eBioMedicine, 2019. DOI: https://doi.org/10.1016/j.ebiom.2018.12.052

Kirkland, J. L., Hollenberg, C. H., & Gillon, W. S. (1990). Age, anatomic site, and the replication and differentiation of adipocyte precursors. *Am J Physiol, 258*(2 Pt 1), C206-210. doi:10.1152/ajpcell.1990.258.2.C206

Kirkland, J. L., & Tchkonia, T. (2015). Clinical strategies and animal models for developing senolytic agents. *Experimental Gerontology, 68*, 19-25. doi:https://doi.org/10.1016/j.exger.2014.10.012

Kirkland, J. L., & Tchkonia, T. (2017). Cellular Senescence: A Translational Perspective. *EBioMedicine, 21*(Supplement C), 21-28. doi:https://doi.org/10.1016/j.ebiom.2017.04.013

Kirkland, J. L., Tchkonia, T., Zhu, Y., Niedernhofer, L. J., & Robbins, P. D. (2017). The Clinical Potential of Senolytic Drugs. *Journal of the American Geriatrics Society, 65*(10), 2297-2301. doi:10.1111/jgs.14969

Krishnamurthy, J., Torrice, C., Ramsey, M. R., Kovalev, G. I., Al-Regaiey, K., Su, L., & Sharpless, N. E. (2004). Ink4a/Arf expression is a biomarker of aging. *The Journal of Clinical Investigation, 114*(9), 1299-1307. doi:10.1172/JCI22475

Lau, A., Kennedy, B.K., Kirkland, J.L., Stefan G. Tullius, S.G. (2019) Mixing old and young: Enhancing rejuvenation and accelerating aging. J. Clin. Invest. 129:4-11. doi: 10.1172/JCI123946.

Lehmann, M., Korfei, M., Mutze, K., Klee, S., Skronska-Wasek, W., Alsafadi, H. N., . . . Königshoff, M. (2017). Senolytic drugs target alveolar epithelial cell function and attenuate experimental lung fibrosis. *European Respiratory Journal, 50*(2). doi:10.1183/13993003.02367-2016

Li, Y., He, L., Huang, X., Issa Bhaloo, S., Zhao, H., Zhang, S., . . . Zhou, B. (2018). Genetic Lineage Tracing of Non-Myocyte Population by Dual Recombinases. *Circulation*. doi:10.1161/circulationaha.118.034250

Mohsin S et al. Rejuvenation of human cardiac progenitor cells with Pim-1 kinase. Circ Res. 2013 Oct 25;113(10):1169-79

Ogrodnik, M., Miwa, S., Tchkonia, T., Tiniakos, D., Wilson, C. L., Lahat, A., . . . Jurk, D. (2017). Cellular senescence drives age-dependent hepatic steatosis. *Nature Communications, 8*, 15691. doi:10.1038/ncomms15691

Ogrodnik, M., Yi Zhu, Y., Prata, L., Tchkonia, T., Krüger, P., Fielder, E., Victorelli, S., Ruswhandi, R.A., Giorgadze, N., Pirtskhalava, T., Podgorni, O., Enikolopov, G., Johnson, K.O., Xu, M., Inman, C., Weigl, M., Ikeno, Y., Burns, T.C., Passos, J.F., von Zglinicki, T., Kirkland, J.L., Jurk, D. Obesity-induced cellular senescence drives anxiety-like behavior and impairment of neurogenesis. Cell Metabolism DOI:https://doi.org/10.1016/j.cmet.2018.12.008

Pajvani, U. B., Trujillo, M. E., Combs, T. P., Iyengar, P., Jelicks, L., Roth, K. A., . . . Scherer, P. E. (2005). Fat apoptosis through targeted activation of caspase 8: a new mouse model of inducible and reversible lipoatrophy. *Nat Med, 11*(7), 797-803. doi:10.1038/nm1262

Roos, C. M., Zhang, B., Palmer, A. K., Ogrodnik, M. B., Pirtskhalava, T., Thalji, N. M., . . . Miller, J. D. (2016). Chronic senolytic treatment alleviates established vasomotor dysfunction in aged or atherosclerotic mice. *Aging Cell, 15*(5), 973-977. doi:10.1111/acel.12458

Schafer, M. J., White, T. A., Iijima, K., Haak, A. J., Ligresti, G., Atkinson, E. J., . . . LeBrasseur, N. K. (2017). Cellular senescence mediates fibrotic pulmonary disease. *Nature Communications, 8*, 14532. doi:10.1038/ncomms14532

Sharpless, N. E., & DePinho, R. A. (2007). How stem cells age and why this makes us grow old. *Nature Reviews Molecular Cell Biology, 8*, 703. doi:10.1038/nrm2241

Formatted: Font: Not Bold, Highlight

Smith, A. J., Lewis, F. C., Aquila, I., Waring, C. D., Nocera, A., Agosti, V., . . . Ellison, G. M. (2014). Isolation and Characterization of Resident Endogenous c-Kit+ Cardiac Stem Cells from the Adult Mouse and Rat Heart. *Nature Protocols, 9*, 1662. doi:10.1038/nprot.2014.113

St Sauver, J. L., Boyd, C. M., Grossardt, B. R., Bobo, W. V., Finney Rutten, L. J., Roger, V. L., . . . Rocca, W. A. (2015). Risk of developing multimorbidity across all ages in an historical cohort study: differences by sex and ethnicity. *BMJ Open, 5*(2). doi:10.1136/bmjopen-2014-006413

Tang, X. L., Li, Q., Rokosh, G., Sanganalmath, S. K., Chen, N., Ou, Q., . . . Bolli, R. (2016). Long-Term Outcome of Administration of c-kit(POS) Cardiac Progenitor Cells After Acute Myocardial Infarction: Transplanted Cells Do not Become Cardiomyocytes, but Structural and Functional Improvement and Proliferation of Endogenous Cells Persist for at Least One Year. *Circ Res, 118*(7), 1091-1105. doi:10.1161/circresaha.115.307647

Tchkonia, T., & Kirkland, J. L. (2018). Aging, Cell Senescence, and Chronic Disease: Emerging Therapeutic Strategies. *Jama, 320*(13), 1319-1320. doi:10.1001/jama.2018.12440

Tchkonia, T., Zhu, Y., van Deursen, J., Campisi, J., & Kirkland, J. L. (2013). Cellular senescence and the senescent secretory phenotype: therapeutic opportunities. *The Journal of Clinical Investigation, 123*(3), 966-972. doi:10.1172/JCI64098

Torella, D., Ellison, G. M., Karakikes, I., & Nadal-Ginard, B. (2007). Resident cardiac stem cells. *Cell Mol Life Sci, 64*(6), 661-673. doi:10.1007/s00018-007-6519-y

Torella, D., Rota, M., Nurzynska, D., Musso, E., Monsen, A., Shiraishi, I., . . . Leri, A. (2004). Cardiac Stem Cell and Myocyte Aging, Heart Failure, and Insulin-Like Growth Factor-1 Overexpression. *Circulation Research, 94*(4), 514. doi:10.1161/01.RES.0000117306.10142.50

van Berlo, J. H., Kanisicak, O., Maillet, M., Vagnozzi, R. J., Karch, J., Lin, S. C., . . . Molkentin, J. D. (2014). c-kit+ cells minimally contribute cardiomyocytes to the heart. *Nature, 509*(7500), 337-341. doi:10.1038/nature13309

Vicinanza, C., Aquila, I., Cianflone, E., Scalise, M., Marino, F., Mancuso, T., . . . Torella, D. (2018). Kitcre knock-in mice fail to fate-map cardiac stem cells. *Nature, 555*, E1. doi:10.1038/nature25771

Vicinanza, C., Aquila, I., Scalise, M., Cristiano, F., Marino, F., Cianflone, E., . . . Torella, D. (2017). Adult Cardiac Stem Cells are Multipotent and Robustly Myogenic: C-kit Expression is Necessary but not Sufficient for their Identification. *Cell Death And Differentiation, 24*, 2101. doi:10.1038/cdd.2017.130

Xu, M., Palmer, A. K., Ding, H., Weivoda, M. M., Pirtskhalava, T., White, T. A., . . . Kirkland, J. L. (2015). Targeting senescent cells enhances adipogenesis and metabolic function in old age. *eLife, 4*, e12997. doi:10.7554/eLife.12997

Xu, M., Pirtskhalava, T., Farr, J. N., Weigand, B. M., Palmer, A. K., Weivoda, M. M., . . . Kirkland, J. L. (2018). Senolytics improve physical function and increase lifespan in old age. *Nature Medicine*. doi:10.1038/s41591-018-0092-9

Xu, M., Tchkonia, T., Ding, H., Ogrodnik, M., Lubbers, E. R., Pirtskhalava, T., . . . Kirkland, J. L. (2015). JAK inhibition alleviates the cellular senescence-associated secretory phenotype and frailty in old age. *Proceedings of the National Academy of Sciences, 112*(46), E6301-E6310. doi:10.1073/pnas.1515386112

Zhu, Y., Tchkonia, T., Pirtskhalava, T., Gower, A. C., Ding, H., Giorgadze, N., . . . Kirkland, J. L. (2015). The Achilles' heel of senescent cells: from transcriptome to senolytic drugs. *Aging Cell, 14*(4), 644-658. doi:10.1111/acel.12344

Supporting Information listing

Extended experimental procedures
Tables S1 – S3
Figures S1 – S10

Figure. 1. Over half of CPCs in the aged human heart are senescent (**a**) Representative immunofluorescence images and quantification of c-kit^{pos} p16^{INK4Apos} CPCs, (n=35 donors~~2~~), (**b**) c-kit^{pos} SA-β-gal^{pos} CPCs (**P*=0.0014; n=2-4), (**c**) c-kit^{pos} γ-H2AX^{pos} p16^{INK4A}-expressing CPCs (**P*=0.0264; n=5 donors). (**d**) Q-FISH telomere length of single c-kit^{pos} CPCs (n=100 cells per group, 20 cells per donor). Representative immunofluorescence images of telomere staining, L5178Y-S (10 Kb) and L5178Y-R (79 Kb) are mouse cell lines with known telomere length. Frequency distribution histogram of CPC telomere length (n=5 donors/group). Nuclei stained in blue by DAPI. All data are Mean ± SEM.

Figure. 2. CPCs isolated from aged hearts exhibit diminished proliferation, clonogenicity, and cardiomyocyte differentiation potential (**a**) Quantification of CPC proliferation (**P*=0.0266; n=3-4 donors), (**b**) single CPC-derived clonal efficiency (**P*=0.0008, n=4-5 donors), (**c**) CPC spherogenesis number (**P*=0.0051) and (**d**) size (**P*=0.01), (n=2-3 donors). (**e**) Representative immunofluorescence images of undifferentiated and differentiated CPCs from old and middle-aged donors. Nuclei stained in blue by DAPI. (**f**) Quantification of Nkx2.5^{pos} (**P*=0.0295; n=3 donors~~2~~), and (**g**) α-sarcomeric actin expression (**P*=0.023; n=~~2~~ 3 donors). All data are Mean ± SEM.

Formatted: Highlight
Formatted: Highlight

Figure. 3. Aged-senescent CPCs show decreased reparative potential (**a**) *In vivo* MI experimental design. (**b**) Representative confocal images of PKH26^{pos} CPCs engrafted in the myocardium 4 days post-MI. (**c**) Quantification and representative confocal images of engraftment of PKH26^{pos} cells 28 days post-MI (**P*=0.015 *vs*. c-kit^{neg} cells, n=4-5 mice). (**d**) Echocardiography measurements of LV ejection fraction (EF), fractional shortening (FS), left ventricular end-diastolic diameter (LVEDD), and left ventricular end-systolic diameter (LVESD) at baseline (BL) before MI, 7 and 28 days after MI and cell injection (**P*<0.05 *vs*. Sham, †*P*<0.05 *vs*. Cycling-CPCs, Δ*P*<0.05 *vs*. dox-induced Sen-CPCs, n=5-7 mice). (**e**) Representative micrographs and quantification of average LV fibrosis (**P*<0.05 *vs*. Sham; †*P*=0.0112 *vs*. Cycling-CPCs; n=5-6 mice). (**f**) Representative confocal images of PKH26 co-expression with α-sarcomeric actinin and vWF (arrowheads) 28 days post-MI. (**g**) Quantification and representative confocal images of BrdU^{pos}/α-sarcomeric actinin^{pos} cardiomyocytes and BrdU^{pos}/vWF^{pos} capillaries (**P*<0.05 *vs*. all; n=5-7 mice). Nuclei stained in blue by DAPI. All data are Mean ± SEM.

Figure. 4. Aged-senescent CPCs have a SASP (**a**) Transcript SASP factor expression of dox-induced Sen-CPCs relative to Cycling-CPCs (control). (**b**) SASP factor protein levels quantified by Luminex of unconditioned media (UM), Cycling- CPC (CM) and dox-induced Sen-CPC (Sen CM) conditioned media (**P*<0.05 *vs*. UM and CM). Conditioned media

Formatted: Font: Italic

applied to cycling-competent CPCs and the following analyses performed; (**c**) Quantification and representative staining of CPC proliferation (**P*<0.001; n=5 replicates), (**d**) $p16^{INK4A\text{-}pos}$ CPCs (**P*<0.0001; n=5 replicates), (**e**) SA-β-gal^{pos} CPCs (**P*<0.0001; n=5 replicates), (**f**) γH2AX^{pos} CPCs (**P*<0.001; n=5 replicates). All data are Mean ± SEM.

Figure. 5. Senolytic clearance abrogates the SASP (**a**) Viability (Crystal violet) and SA-β-gal quantification of dox-induced Sen-CPCs and Cycling-CPCs exposed to various concentrations of D+Q for 3 days. (**b-f**) Quantification of 7 days of co-culture of Cycling-CPCs with dox-induced Sen-CPCs for (**b**) viability (**P*=0.0068); (**c**) proliferation (**P*=0.0056); (**d**) $p16^{INK4A}$ (**P*=0.0025); (**e**) SA-β-gal (**P*=0.0025); (**f**) γH2AX (**P*=0.0002). CTRL is Cycling- CPCs alone. (n=5 replicates). ~~Data are Mean ± SEM.~~ (**g**) Representative SA-β-gal staining after clearance of dox-induced Sen-CPCs from co-culture by D+Q treatment. (**h-k**) Quantification of 17 days of co-culture of Cycling-CPCs with dox-induced Sen-CPCs or co-culture with D+Q treatment for (**h**) viability (**P*<0.0001 *vs*. CTRL 17d; †*P*=0.0001 *vs*. co-culture 17d); (**i**) proliferation (**P*<0.0001 *vs*. CTRL 17d; †*P*<0.0001 *vs*. co-culture 17d); (**j**) $p16^{INK4A}$ (**P*<0.0001 *vs*. CTRL 17d; †*P*<0.0001 *vs*. co-culture 17d) and (**k**) SA-β-gal (**P*<0.0001 *vs*. CTRL 17d; †*P*<0.0001 *vs*. co-culture 17d). CTRL is Cycling-CPCs alone. (n=5 replicates). (**l**) SASP factor protein levels quantified by Luminex from each treatment condition (**P*<0.0001 *vs*. CTRL; †*P*<0.01 *vs*. co-culture 7d and 17d). (n=2 replicates). All data are Mean ± SEM.

Figure. 6. Clearance of senescent cells stimulates new cardiomyocyte formation ~~in~~ in the aged heart (**a**) *In vivo* senescent cell clearance experimental design. (**b**) Total cardiac $p16^{Ink4a}$ gene expression following clearance (**P*<0.01 *vs*. Vehicle; n=5 mice). (**c**) Quantification of CPCs following clearance, (**P*<0.0001 *vs*. Vehicle; †*P*=0.0453 *vs*. AP; n=10-11 mice). (**d**) Frequency distribution histogram of cardiomyocyte diameter, (n=6 mice). (**e**) A Ki67^{pos}/α-sarcomeric actin^{pos} cardiomyocyte (arrowhead) in the LV of a 32 month D+Q-treated mouse. (**f**) Quantification of Ki67^{pos} cardiomyocytes, (**P*<0.0001 *vs*. Vehicle; n=10 mice). (**g**) An EdU^{pos}/α-sarcomeric actin^{pos} cardiomyocyte in the LV of a 22 month INK-ATTAC AP-treated mouse. Nuclei are stained by DAPI in blue. (**h**) Quantification of EdU^{pos} cardiomyocytes (**P*<0.0001 *vs*. Old+Vehicle; †*P*<0.0001 *vs*. Young+AP; n=5 mice). (**i**) Quantification of LV fibrosis (**P*<0.05 *vs*. Vehicle; n=3 mice). All data are Mean ± SD.

Formatted: Font: Italic

Figure 1

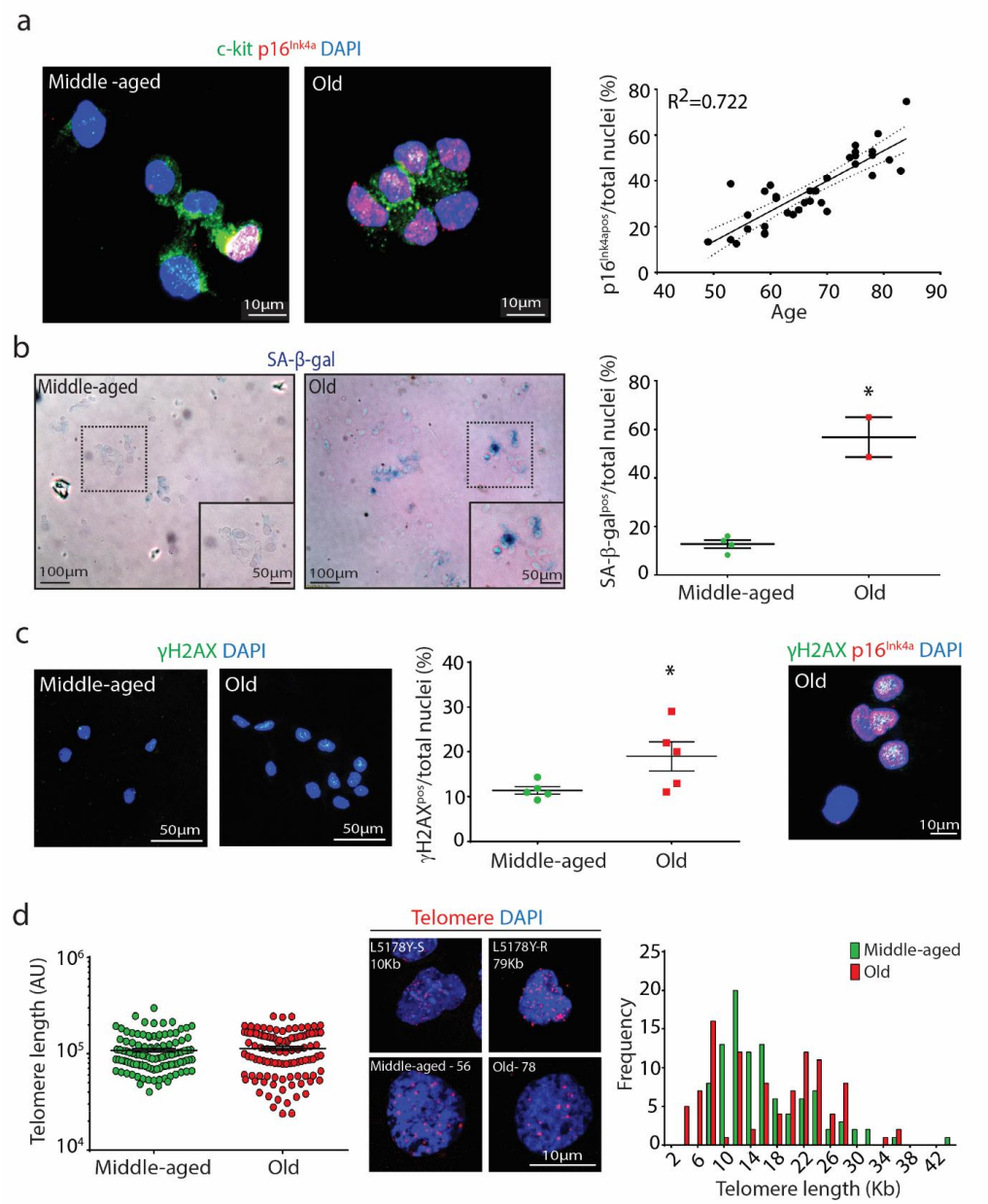
a
c-kit p16Ink4a DAPI
Middle -aged
Old
10µm
10µm
R2=0.722
p16Ink4apos/total nuclei (%)
Age
b
SA-β-gal
Middle-aged
Old
100µm
50µm
100µm
50µm
SA-β-galpos/total nuclei (%)
Middle-aged
Old
c
γH2AX DAPI
Middle-aged
Old
50µm
50µm
γH2AXpos/total nuclei (%)
Middle-aged
Old
γH2AX p16Ink4a DAPI
Old
10µm
d
Telomere length (AU)
Middle-aged
Old
Telomere DAPI
L5178Y-S
10Kb
L5178Y-R
79Kb
Middle-aged - 56
Old- 78
10µm
Middle-aged
Old
Frequency
Telomere length (Kb)

Figure 2

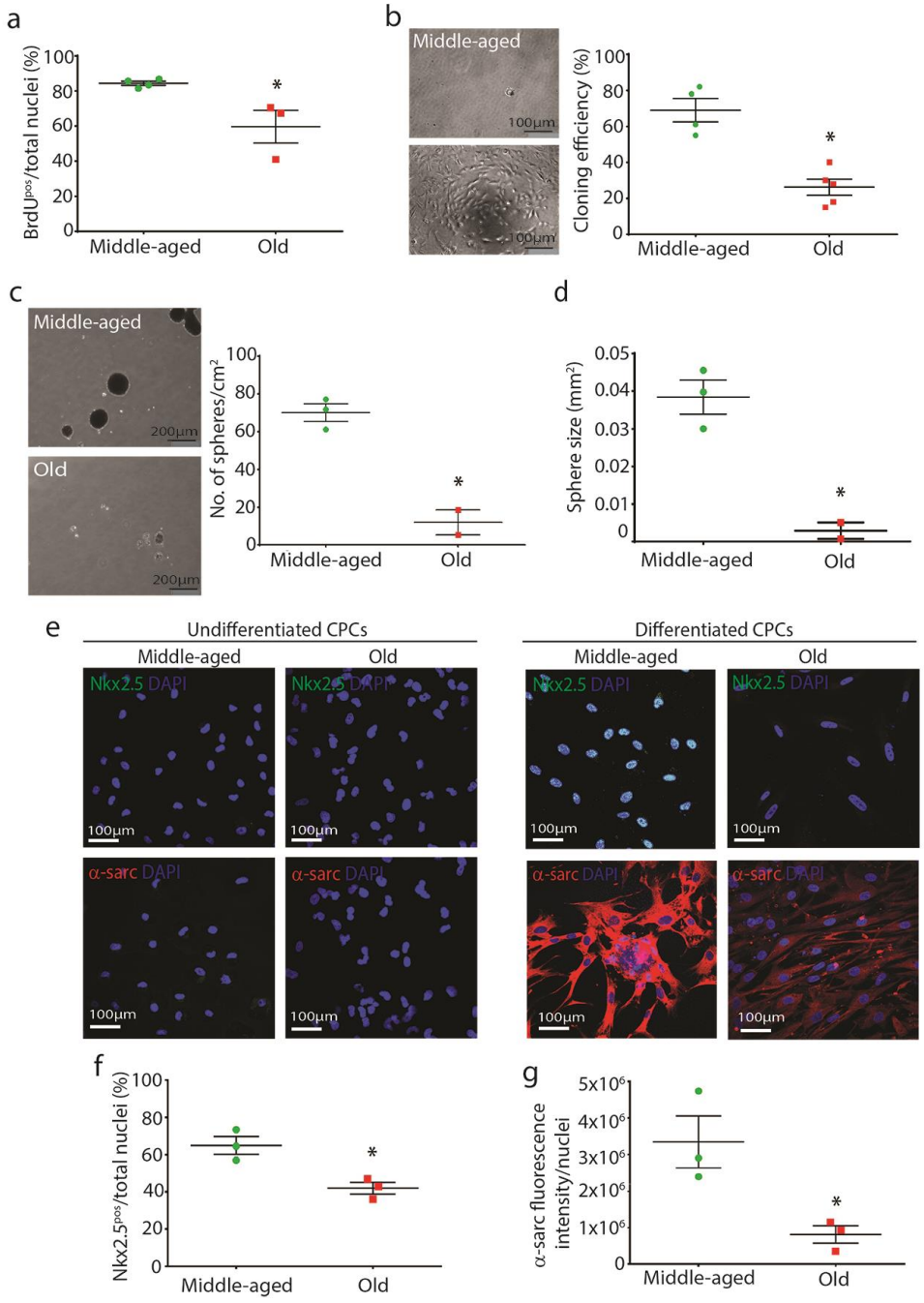
a
BrdU^pos/total nuclei (%)
100
80
60
40
20
0
*
Middle-aged
Old
b
Middle-aged
100µm
100µm
Cloning efficiency (%)
100
80
60
40
20
0
*
Middle-aged
Old
c
Middle-aged
200µm
Old
200µm
No. of spheres/cm²
100
80
60
40
20
0
*
Middle-aged
Old
d
Sphere size (mm²)
0.05
0.04
0.03
0.02
0.01
0
*
Middle-aged
Old
e
Undifferentiated CPCs
Differentiated CPCs
Middle-aged
Old
Middle-aged
Old
Nkx2.5 DAPI
α-sarc DAPI
100µm
f
Nkx2.5^pos/total nuclei (%)
100
80
60
40
20
0
*
Middle-aged
Old
g
α-sarc fluorescence intensity/nuclei
5x10⁶
4x10⁶
3x10⁶
2x10⁶
1x10⁶
0
*
Middle-aged
Old

Figure 3

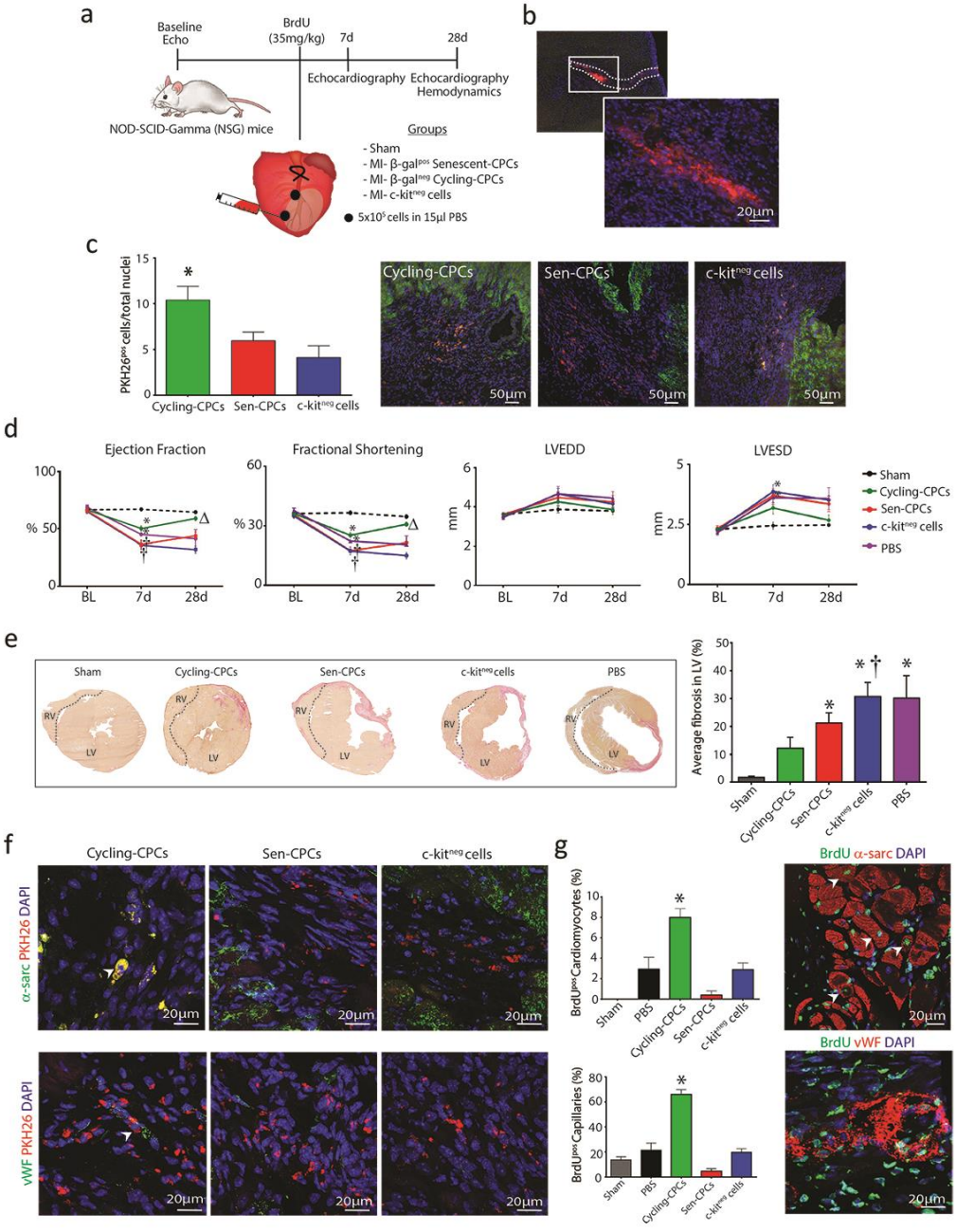

Figure 4

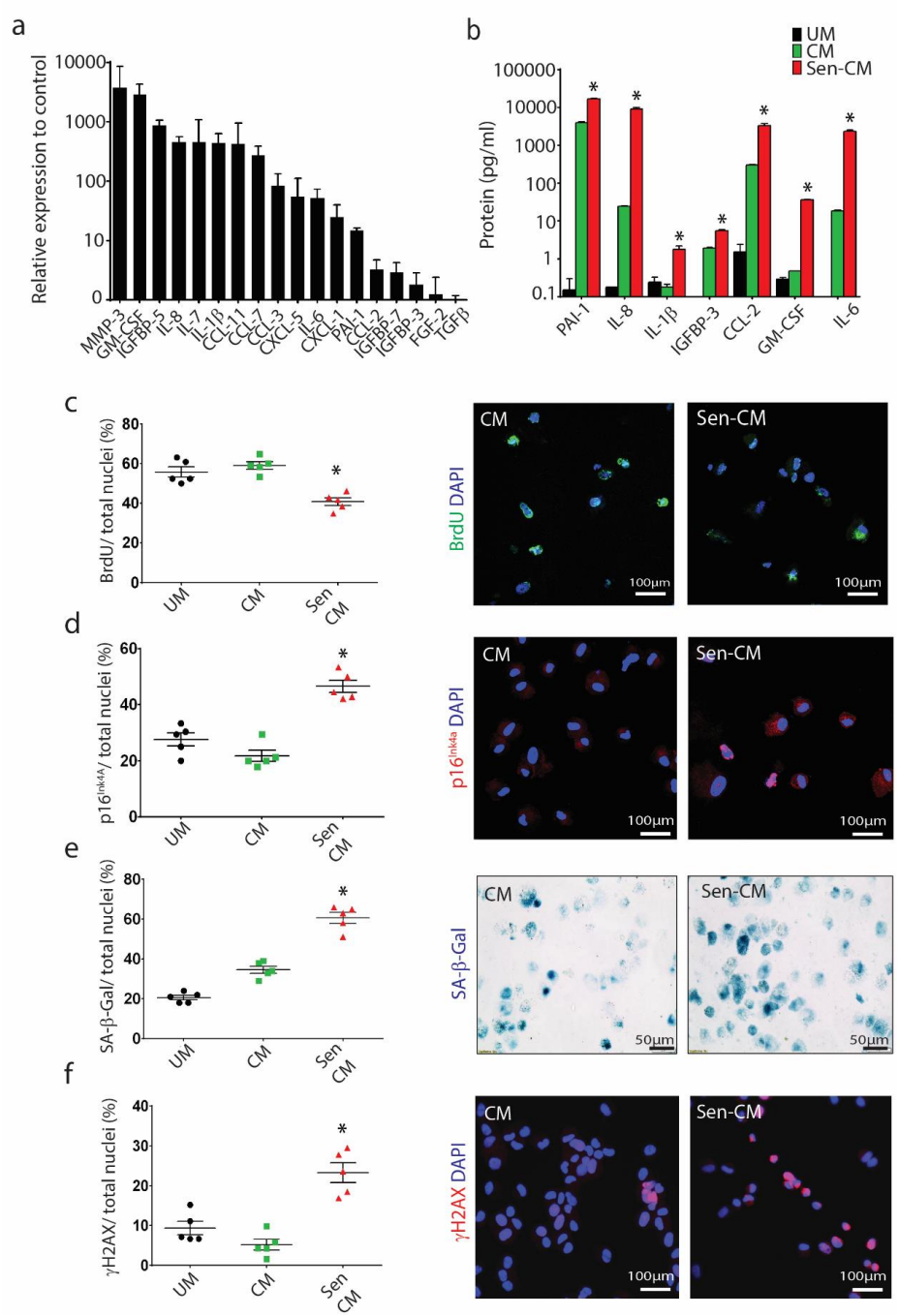
a
Relative expression to control
MMP-3
GM-CSF
IGFBP-5
IL-8
IL-7
IL-1β
CCL-11
CCL-7
CCL-3
CXCL-5
IL-6
CXCL-1
PAI-1
CCL-2
IGFBP-7
IGFBP-3
FGF-2
TGFβ
b
UM
CM
Sen-CM
Protein (pg/ml)
PAI-1
IL-8
IL-1β
IGFBP-3
CCL-2
GM-CSF
IL-6
c
BrdU/ total nuclei (%)
UM
CM
Sen CM
BrdU DAPI
CM
Sen-CM
100μm
d
p16Ink4A/ total nuclei (%)
p16Ink4a DAPI
e
SA-β-Gal/ total nuclei (%)
SA-β-Gal
50μm
f
γH2AX/ total nuclei (%)
γH2AX DAPI

Figure 5

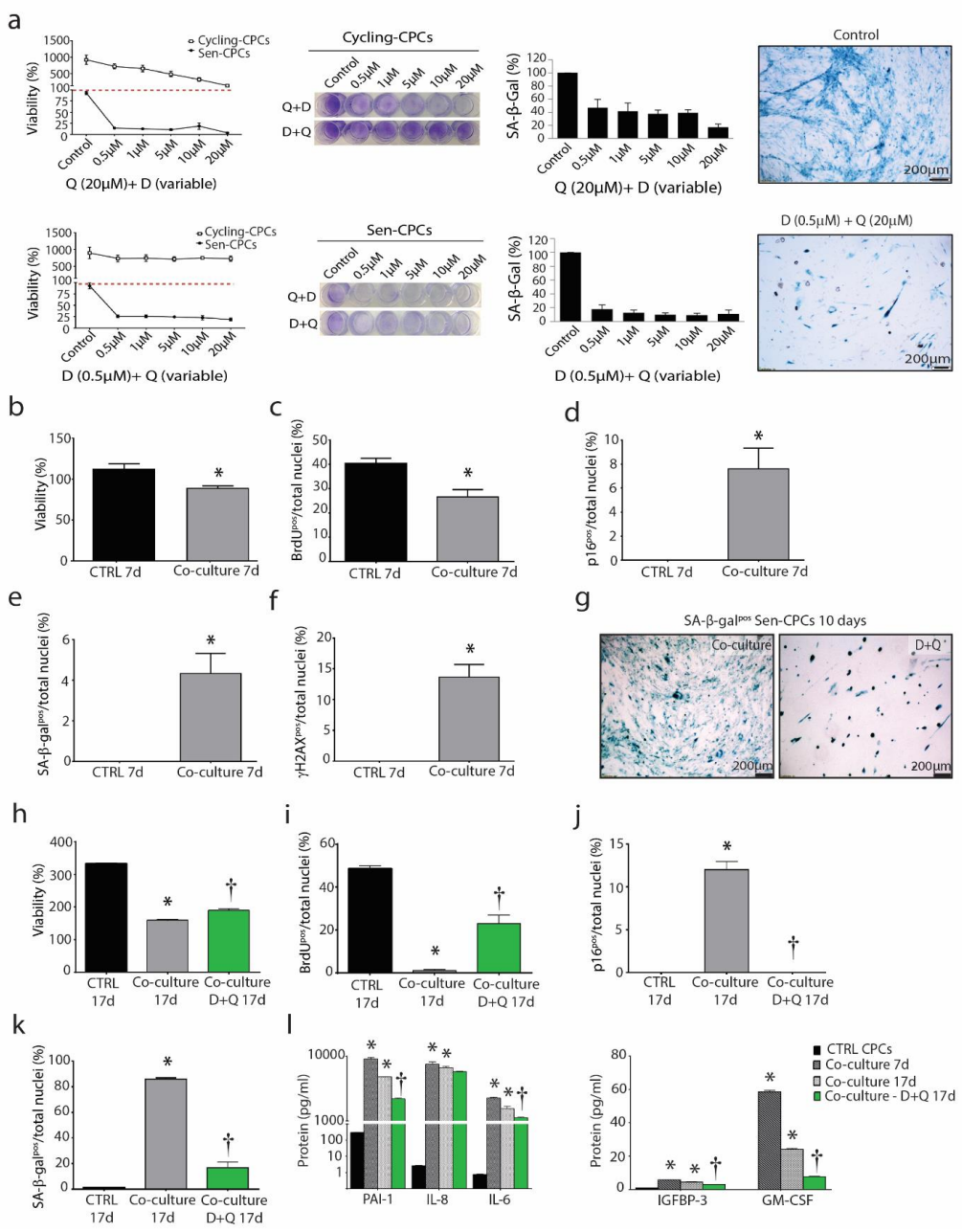
a
Cycling-CPCs
Sen-CPCs
Viability (%)
Control
0.5µM
1µM
5µM
10µM
20µM
Q (20µM)+ D (variable)
Q+D
D+Q
SA-β-Gal (%)
Control
200µm
D (0.5µM)+ Q (variable)
D (0.5µM) + Q (20µM)
b
Viability (%)
CTRL 7d
Co-culture 7d
c
BrdU^pos/total nuclei (%)
d
p16^pos/total nuclei (%)
e
SA-β-gal^pos/total nuclei (%)
f
γH2AX^pos/total nuclei (%)
g
SA-β-gal^pos Sen-CPCs 10 days
Co-culture
D+Q
h
CTRL 17d
Co-culture 17d
Co-culture D+Q 17d
i
j
k
l
Protein (pg/ml)
PAI-1
IL-8
IL-6
IGFBP-3
GM-CSF
CTRL CPCs
Co-culture 7d
Co-culture 17d
Co-culture - D+Q 17d

Figure 6

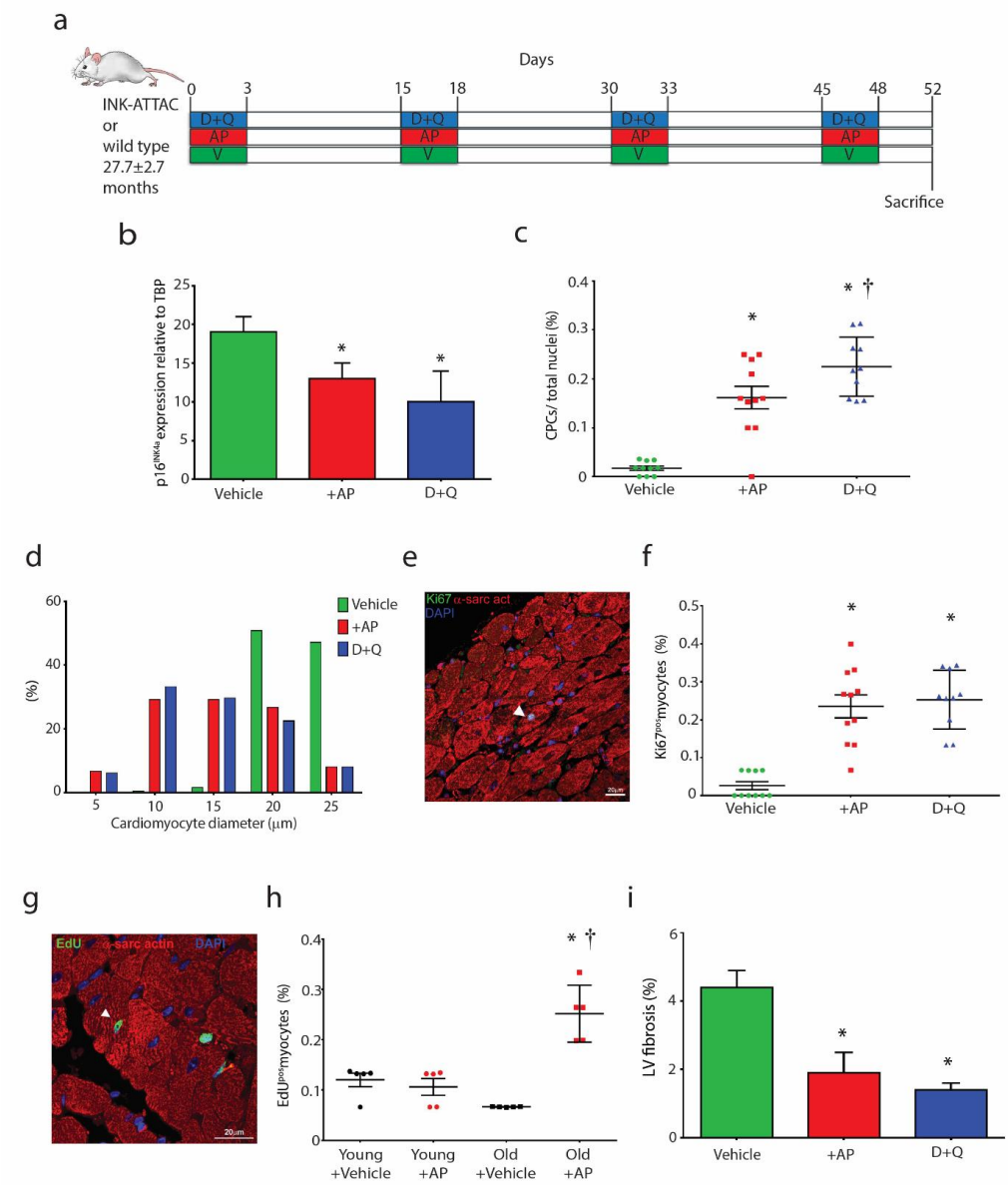
a
Days
0
3
15
18
30
33
45
48
52
INK-ATTAC
or
wild type
27.7±2.7
months
D+Q
AP
V
Sacrifice
b
p16INK4a expression relative to TBP
Vehicle
+AP
D+Q
c
CPCs/ total nuclei (%)
Vehicle
+AP
D+Q
d
(%)
Vehicle
+AP
D+Q
Cardiomyocyte diameter (μm)
e
Ki67 α-sarc act
DAPI
f
Ki67POSmyocytes (%)
Vehicle
+AP
D+Q
g
EdU
α-sarc actin
DAPI
h
EdUPOSmyocytes (%)
Young
+Vehicle
Young
+AP
Old
+Vehicle
Old
+AP
i
LV fibrosis (%)
Vehicle
+AP
D+Q